A band theoretical explanation for the electronic specific heat of some copper–gold alloys

K Kokko, E Ojala and K Mansikka

Department of Physical Sciences, University of Turku, SF-20500 Turku, Finland

Abstract. The low temperature electronic specific heat as a function of Au content in Cu–Au alloys shows interesting features. The specific heat coefficient of disordered alloys lies on a smooth curve below the linearly interpolated elemental metal values. Ordering reduces the value of this coefficient in all cases except that of the CuAu I alloy. It is shown that this behaviour of the electronic specific heat is due to the specific structure of the electronic density of states around the Fermi level. The position and shape of the large dip we found at the Fermi level varies with changes in the chemical composition or the crystal structure of the alloy. The singular property of the specific heat of CuAu I can be explained by the lattice contraction in the c direction. Besides these Fermi level properties, the electron density of occupied states, resolved into the total and Au part, is discussed for the case of Cu_3Au I, CuAu I and $CuAu_3$. Characteristic d-band energies (top, centre and bottom) are also presented. The calculations were performed using the linear-muffin-tin-orbital method.

1. Introduction

According to experiments the low temperature electronic specific heat coefficient (γ) of disordered Cu–Au alloys lies below the linearly interpolated elemental metal values. Ordering, however, changes the specific heat value appreciably [1]. In this study the electronic density of states (DOS) of some ordered Cu–Au alloys was calculated. These data were then analysed in order to determine the effects of chemical composition and crystal structure on the electronic properties of Cu–Au alloys. It is shown that the behaviour of the electronic specific heat of these alloys is due to the specific structure of the DOS around the Fermi level.

At high temperatures Cu and Au form a continuous disordered solid solution based upon the FCC structure, while at lower temperatures there are five ordered phases in the alloy system: Cu_3Au I, Cu_3Au II, CuAu I, CuAu II and $CuAu_3$. Cu_3Au I has a cubic $L1_2$ type structure, CuAu I has a tetragonal $L1_0$ type structure, Cu_3Au II, CuAu II and $CuAu_3$ have a long period anti-phase domain structure [2–5]. In the following the main interest will be in the ordered phases of Cu_3Au I and CuAu I, but disordered alloys will also be discussed.

2. Calculations

The calculations were performed using the self-consistent-field linear-muffin-tin-orbital (LMTO) method [6, 7], including the combined correction terms in the scalar relativistic

form and using the so called atomic sphere approximation. The basis function set for the valence electrons consisted of s-, p- and d-functions. The exchange-correlation effects were introduced within the local-density approximation using the Barth–Hedin potential [8]. The core states were determined by self-consistent-field fully relativistic calculations and were held fixed throughout the self-consistent cycles of the valence electrons. The ratio of Cu and Au Wigner–Seitz radii of the alloys was taken to be the same as for elemental Cu and Au metals. Calculations were also performed using atomic Wigner–Seitz radii of equal size for both Cu and Au atoms, to check the sensitivity of the results to this kind of numerical effect. It was found that the total DOS at the Fermi level ($N(E_F)$) in the latter case was about one per cent higher than in the former, a shift, however, smaller by an order of magnitude than the typical differences in $N(E_F)$ between different phases of Cu–Au alloys. The last iterations in each self-consistent cycle were performed on a grid corresponding to 680 and 910 k-points in the irreducible wedge of the Brillouin zone of Cu_3Au I and CuAu I respectively. The lattice parameters were $a = 3.6147$ Å and 4.07833 Å for elemental Cu and Au, respectively, $a = 3.7426$ Å for Cu_3Au I, $a = 3.966$ Å and $c/a = 0.9251$ for CuAu I and $a = 3.9820$ Å for $CuAu_3$, which was calculated in the hypothetical $L1_2$ structure.

3. Results and discussion

3.1. General features of the DOS

The present results agree quite well with other self-consistent-field calculations for Cu_3Au I. Agreement for instance with the scalar-relativistic LAPW results of Wertheim *et al* [9] is good (with differences in the positions of the main DOS peaks typically of the order of 0.1 eV). When the present results are compared to the fully relativistic LMTO results of Weinberger *et al* [10] the agreement in the Cu part of the DOS is good (with differences of the order of 0.1 eV). In the Au part of the DOS, on the other hand, there are greater differences, due to the appreciable spin-orbit splitting of the Au bands. The calculated DOS of Cu_3Au I is also in close agreement with the photoemission measurements of Eberhardt *et al* [11], Di Cenzo *et al* [12] and Wertheim *et al* [9], if the Fermi level shift of 0.7 eV (discussed below) is taken into account.

The calculated total DOS of some ordered Cu–Au alloys are shown in figure 1. At the middle of the d-band of Cu_3Au I there is a dip, dividing the band structure into two distinct parts: a lower part mainly of Au type and an upper part mainly of Cu type. Although this division into Au and Cu parts is not as apparent in CuAu I and $CuAu_3$ as in Cu_3Au I, it is nevertheless discernible.

The main characteristics of the DOS depend appreciably on the compositions of the alloys. As the Au content increases the Au part broadens and the Cu part becomes narrower. The width of the Cu part compared to the corresponding elemental metal d-band width is about 70%, 60% and 30% for Cu_3Au I, CuAu I and $CuAu_3$ respectively. For the Au part the corresponding values are approximately 50%, 60% and 80%. This behaviour is an indication of changes in the overlapping of the d states. As the Au content increases the overlapping of the Au d states increases and that of the Cu d states decreases. While the composition of the alloys has a dramatic effect on the distribution of the d states, the change in the c/a ratio from 1 to 0.9251 in CuAu I has only a minor effect on the general appearance of the DOS.

Before the discussion of band energies, it should be noted that the d-band binding energies of noble metals obtained by several recent self-consistent-field calculations tend
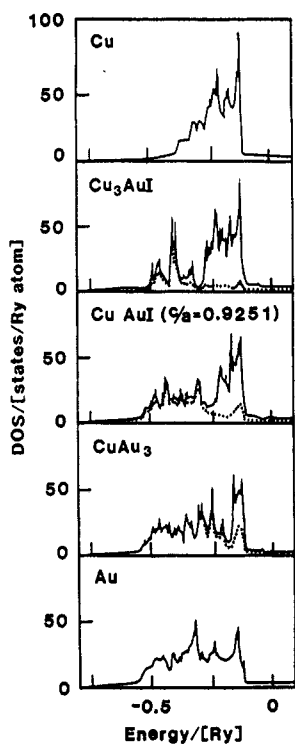
Figure 1. Electronic density of states for some ordered Cu–Au alloys and elemental Cu and Au. In addition to total density of states (full curve) Au component (broken curve) are also shown. The origin is located at the Fermi energy.

Table 1. Characteristic d-band energies relative to the Fermi energy: top (A), centre (C) and bottom (B); total electronic density of states at the Fermi level ($N(E_F)$), and the corresponding band structure electronic specific heat coefficients (γ_{band}).

	A_{Au} (mRyd)	C_{Au} (mRyd)	B_{Au} (mRyd)	A_{Cu} (mRyd)	C_{Cu} (mRyd)	B_{Cu} (mRyd)	$N(E_F)$ (states Ryd^{-1}/atom)	γ_{band} (mJ mol^{-1} K^{-2})
Cu				−117	−201	−336	4.08	0.707
Cu$_3$Au I	−178	−346	−547	−107	−192	−329	3.85	0.668
CuAu I†	−163	−333	−535	−95	−181	−320	3.32	0.575
CuAu I‡	−165	−334	−536	−96	−182	−320	4.09	0.709
CuAu$_3$	−150	−319	−520	−86	−172	−311	4.13	0.715
Au	−131	−303	−508				3.80	0.659

† $c/a = 1$.
‡ $c/a = 0.9251$.

to be too low [13, 14]. This error, according to Wertheim *et al* [9], is 0.56 eV for Au and 0.65 eV for Cu$_3$Au I. Likewise Weinberger *et al* [10] mention that they had to shift the calculated spectra of Cu$_3$Au I by 0.7 eV towards lower energies in order to obtain agreement with experimental results. The d-band binding energies obtained by the present calculations differ from experimental values by the same order as the above findings. The present calculations predict a band centre shift of the Au d band in Cu$_3$Au I relative to elemental Au of 0.58 eV. This is in reasonable agreement with the LAPW result of 0.43 eV and with the experimental Au 4f core level shift of 0.55 eV [9]. The other characteristic band energies obtained by the present calculations are shown in table 1.
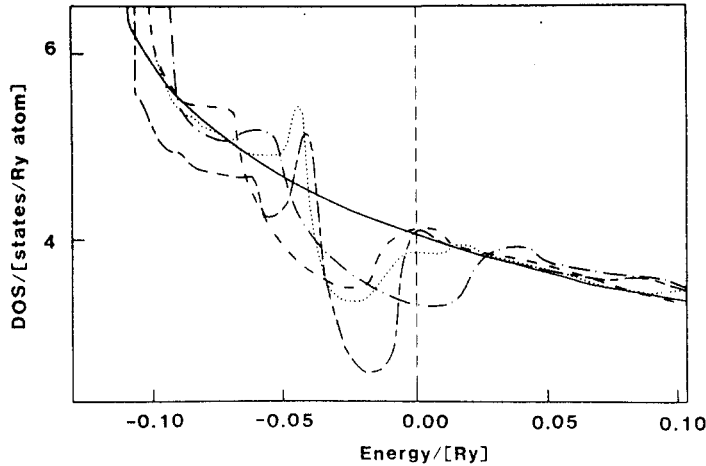
Figure 2. Density of states in the vicinity of the Fermi level. Cu (full curve), Cu_3Au I (dotted curve), CuAu I ($c/a = 0.9251$) (broken curve), CuAu I ($c/a = 1$) (chain-dotted curve) and $CuAu_3$ (chain-broken curve).

In figure 2 the DOS of Cu–Au alloys around the Fermi level are compared to the DOS of elemental Cu. At the Fermi level there is a broad dip in the DOS of Cu–Au alloys. This dip changes with the composition and structure of the alloys. As the Au content increases ($Cu_3Au \rightarrow CuAu$ ($c/a = 1$)), the dip expands, so that its upper edge is lifted above the Fermi level. When the ratio c/a is reduced ($1 \rightarrow 0.9251$), the dip shifts to lower energies and its upper edge drops again below the Fermi level. With an increase in the Au content ($CuAu \rightarrow CuAu_3$) this dip narrows again. These modifications of the shape and position of the dip at the Fermi level have appreciable consequences on the low temperature electronic specific heat.

3.2. Electronic specific heat

The electronic specific heat coefficient γ is related to the electronic density of states at the Fermi level through the equations

$$\gamma = \gamma_{band}(1 + \lambda_{ep} + \lambda_{ee}) \qquad \gamma_{band} = (\pi^2 k_B^2/3)\, N(E_F(0))$$

where k_B is the Boltzmann constant, $E_F(0)$ is the Fermi energy at 0 K, $N(E_F(0))$ is the total DOS at the Fermi level and λ_{ep} and λ_{ee} are the enhancement factors due to electron–phonon and electron–electron interaction, respectively. These equations serve as a link between electronic specific heat measurements and band structure calculations.

Because the value of λ_{ep} for Cu and Au is of about the same order and the value of λ_{ee} is low [15], the effects of these factors on the specific heat are expected to be approximately constant within the whole concentration range. Thus we expect γ_{band} and $\gamma_{band}(1 + \lambda_{ep} + \lambda_{ee})$ to agree in shape and also to a large extent in magnitude.

Before the examination of the results of the calculations, we discuss the comparability of experimental findings and the present theoretical results. Specific heat experiments have been performed at low temperatures, whereas in the calculations experimental room temperature lattice parameters were used. In order to investigate the possible consequences of this temperature difference, a further calculation was performed for elemental Cu using the low temperature lattice parameter $a = 3.5975$ Å. The difference
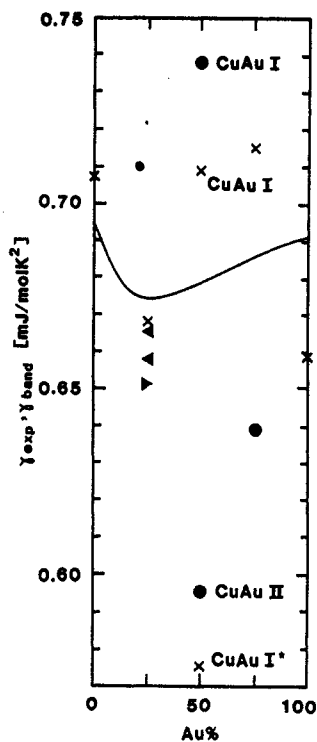
Figure 3. Band structure (γ_{band}) and experimental (γ_{exp}) electronic specific heat coefficient as a function of Au content in Cu–Au alloys. Band structure results are shown by crosses (×), experimental results for disordered alloys are shown by fitted full curve corresponding to measurements of Martin and Waterhouse [1], Martin [16], Delinger *et al* [17], Davis and Rayne [18], Gavignet-Tillard and Hammann [19], Martin [20] and Zrudsky *et al* [21], experimental results for ordered alloys taken from Martin and Waterhouse [1] (●), Martin [16] (▶) and Gavignet-Tillard and Hammann [19] (◀). The CuAu I* corresponds to calculation for CuAu I using the ratio $c/a = 1$.

between the low and room temperature values of $N(E_F)$ proved to be less than one per cent. Furthermore, because this correction to the DOS at the Fermi level is of the same order for all the alloys investigated, it would cause only a small shift in level in the results. Thus if one is interested in the specific heat compared to the elemental Cu value, the greater part of this correction is cancelled out.

Since the effects of spin–orbit interaction appear mainly in the lower part of the d band [10, 13], the exclusion of this interaction in the present calculations would not have any major effect on the total DOS at the Fermi level.

In figure 3 the results of the electronic specific heat measurements [1, 16–21] of Cu–Au alloys in disordered as well as ordered phases are shown. For disordered alloys the experimental electronic specific heat coefficient (γ_{exp}) lies on a smooth curve slightly below the linearly interpolated elemental metal values. Ordering reduces the value of γ_{exp} by a few per cent in all phases except CuAu I, where it is increased. The band structure specific heat coefficient γ_{band} of ordered Cu_3Au I, CuAu I and $CuAu_3$ and elemental Cu and Au is also shown. As figure 3 shows, the theoretical results account well for the trend of the experimental specific heat: the γ_{band} for Cu_3Au I is below and for CuAu I above the linearly interpolated curve. The γ_{band} for $CuAu_3$ is above the elemental metal values, but because the calculated structure does not correspond to the experimentally observed, ordered structure it cannot be compared directly to the measurements. However, the calculated DOS of $CuAu_3$ gives some indication as to why the electronic specific heat coefficient of disordered $CuAu_3$ lies below the elemental metal values. As figure 2 shows, the Fermi level lies on a local maximum of the DOS. Thus disorder smearing will reduce the value of $N(E_F)$ in $CuAu_3$, especially because there is a strong dip just below E_F, and this might lead to the observed trend of γ.

The explanation for the trend of γ in Cu, Cu_3Au I and CuAu I seems to be the specific structure of the DOS at the Fermi level. As figure 2 shows, in Cu_3Au I and CuAu I there

is a broad dip in the DOS around the Fermi level. In Cu_3Au I the position of the dip is such that the $N(E_F)$ is reduced from the elemental Cu value. In CuAu I this dip has shifted to the lower energies: the upper edge of the dip has dropped below the Fermi level and the $N(E_F)$ is elevated above the elemental Cu value.

Martin and Waterhouse [1] suggested that the rather singular property of γ in CuAu I is due to its layered structure. In CuAu I, alternate (002) planes contain either all Cu or all Au atoms, resulting in the contraction in the c direction. In order to investigate the effect of this contraction on the electronic specific heat, another calculation was performed for CuAu I with $c/a = 1$. The results of this calculation are also shown in figures 2 and 3. Figure 3 shows that the contraction in the c direction explains the singular property of γ in CuAu I. According to figure 2 this contraction shifts the dip in the DOS to lower energies, in such a way that $N(E_F)$ is elevated above the elemental Cu value.

Weinberger *et al* [10] mention that the largest changes in the electronic structure of Cu_3Au I upon ordering occur in the energy regions relatively distant from the Fermi level. However, the present calculations suggest that there may also be significant changes around the Fermi level, at least as far as the electronic specific heat is concerned. Figure 2 gives some indications of the reasons for the downward curvature of the experimental specific heat curve in disordered Cu–Au alloys. The dip in the DOS curve around the Fermi level in Cu_3Au I, CuAu I and $CuAu_3$ is rather deep and the DOS outside this dip is only slightly higher than the DOS value in elemental Cu. Disorder smearing will make this DOS relatively smooth, and the smoothed value of the DOS at the Fermi level will be smaller than the corresponding DOS value in elemental Cu.

Disordered Cu–Au alloys are in many respects similar to Ag–Au alloys. For instance both have a downward curvature in the γ-curve. However, there are also some differences between these alloys. The dip in the DOS around the Fermi level in Ag–Au alloys is smaller and lies deeper below the Fermi level than in Cu–Au alloys. This is why the calculated γ for ordered Ag–Au structures seems to account well for the experimentally observed trend of γ in disordered Ag–Au alloys [22]. The fact that the dip in the DOS is greater in Cu–Au than in Ag–Au alloys indicates that Ag and Au atoms are more similar than Cu and Au atoms. This kind of presence in Cu–Au and absence in Ag–Au of the dip at E_F has also been reported by Terakura *et al* [23] in their study of the phase stability of Cu–Ag, Cu–Au and Ag–Au systems.

4. Conclusions

Calculated band structure results were used to interpret the experimental electronic specific heat results of Cu–Au alloys. The present results are in good agreement with experimental as well as other theoretical results. The widths of the Cu and Au parts of the DOS are shown to correlate with the chemical composition of the alloys, whereas the change in c/a in CuAu I has only a minor effect on these widths. The effects of chemical composition on the electronic specific heat in disordered Cu–Au alloys appear in the experimental γ curve, which lies below the linearly interpolated elemental metal values. Ordering reduces the γ-value in all phases except CuAu I, where it is raised. These experimentally observed phenomena are accounted for by the specific structure in the calculated DOS around the Fermi level. There is a dip in the DOS at the Fermi level, the position and shape of which varies with changes in the chemical composition or the crystal structure of the alloy. The value of γ changes depending on the relative position of this dip and the Fermi level. The singular behaviour of γ in CuAu I is shown to be

due to the lattice contraction in the c direction. Careful ultra-violet photoemission measurements (UPS) should reveal these fine details of the DOS near E_F if they exist.

Acknowledgment

References

[1] Martin D L and Waterhouse N 1970 *Can. J. Phys.* **48** 1217
[2] Watanabe D and Fisher P M J 1965 *J. Phys. Soc. Japan* **20** 2170
[3] Massalski T B 1970 *Physical Metallurgy* ed R W Cahn (Amsterdam: North-Holland) ch 4
[4] Pearson W B 1958 *A Handbook of Lattice Spacings and Structures of Metals and Alloys (International Series of Monographs on Metal Physics and Physical Metallurgy 4)* ed G V Raynor (Belfast: Pergamon)
[5] Eckerlin P and Kandler H 1971 *Landolt–Börnstein New Series Group III*, vol 6, ed K-H Hellwege and A M Hellwege (Berlin: Springer)
[6] Andersen O K 1975 *Phys. Rev.* B **12** 3060
[7] Skriver H L 1984 *The LMTO Method (Springer Series in Solid-State Sciences 41)* ed M Cardona and P Fulde (Berlin: Springer)
[8] von Barth U and Hedin L 1972 *J. Phys. C: Solid State Phys.* **5** 1629
[9] Wertheim G K, Mattheiss L F and Buchanan D N E 1988 *Phys. Rev.* B **38** 5988
[10] Weinberger P, Boring A M, Albers R C and Temmerman W M 1988 *Phys. Rev.* B **38** 5357
[11] Eberhardt W, Wu S C, Garrett R, Sondericker D and Jona F 1985 *Phys. Rev.* B **31** 8285
[12] Di Cenzo S B, Citrin P H, Hartford E H and Wertheim G K 1986 *Phys. Rev.* B **34** 1343
[13] MacDonald A H, Daams J M, Vosko S H and Koelling D D 1982 *Phys. Rev.* B **25** 713
[14] Courths R and Hüfner S 1984 *Phys. Rep.* **112** 53
[15] Grimvall G 1981 *The Electron-Phonon Interaction in Metals (Selected Topics in Solid State Physics XVI)* ed E P Wohlfarth (Amsterdam: North-Holland)
[16] Martin D L 1968 *Can. J. Phys.* **46** 923
[17] Delinger W G, Savage W R and Schweitzer J W 1972 *Phys. Rev.* B **6** 338
[18] Davis T H and Rayne J A 1972 *Phys. Rev.* B **6** 2931
[19] Gavignet-Tillard A and Hammann J 1971 *Phys. Lett.* A **37** 93
[20] Martin D L 1968 *Phys. Rev.* **170** 650
[21] Zrudsky D R, Delinger W G, Savage W R and Schweitzer J W 1971 *Phys. Rev.* B **3** 3025
[22] Kokko K, Ojala E and Mansikka K 1989 *Phys. Status Solidi* b **153** 235
[23] Terakura K, Oguchi T, Mohri T and Watanabe K 1987 *Phys. Rev.* B **35** 2169